Performance Simulation and Powertrain Selection for an Electric Drift Trike Vehicle

By

Joshua S. Rohrbaugh

Submitted to the Department of Mechanical Engineering in Partial Fulfillment of the Requirements for the Degree of

Bachelor of Science

at the

Massachusetts Institute of Technology

June 2023



Authored by: Joshua S. Rohrbaugh
Department of Mechanical Engineering
May 12, 2022

Certified by: K. Jack Whipple
Technical Instructor at MIT D-Lab
Thesis Supervisor

Accepted by: Kenneth Kamrin
Associate Professor of Mechanical Engineering
Undergraduate Officer

Performance Simulation and Powertrain Selection for an Electric Drift Trike Vehicle

by

Joshua Rohrbaugh

Submitted to the Department of Mechanical Engineering on May 12, 2022 in Partial Fulfillment of the Requirements for the Degree of Bachelor of Science in Mechanical Engineering

# Abstract

The design process for an Electric Drift Trike Vehicle is examined. Functional requirements and performance specifications for the trike are created. Driving geometrical relations for the trike's frame are set based on experiments in rider posture and comfort. The coefficient of friction for the drive wheels is measured to inform powertrain design decisions. Acceleration profiles of the trike are simulated to select a motor and chain drive ratio for the vehicle. A motor controller and battery system are selected to match the requirements of the drive motor. System architecture and safety features of the trike's electrical system are explained through the startup sequence and wiring diagram of the trike.

Thesis Supervisor: K. Jack Whipple

Title: Technical Instructor at MIT D-Lab

# Acknowledgements

Many thanks to Gabriella Ulloa, Lachtu Vu, and Frank Gonzalez for their contributions to the design and fabrication of trike parts; Jarrod Smith, Roberto Melendez, Jesse George-Akpenyi, and Aditya Mehotra for their mentorship in design of the trike, and thesis content; Daniel Frey, Sandra Lipnoski, and Chris Mayer for their support of the MIT Electric Vehicle Team; Chris Haynes and Pat Mcatamney for their assistance in fabrication, Damian Harty for consultation in vehicle dynamics; Tim Hurd and Roger Lin for donation of batteries. A special thanks to my thesis advisor and project mentor, Jack Whipple.

# Table of Contents

# List of Figures

# List of Tables

# Introduction

## Background

A drift trike is a special variant of tricycle which uses low traction rear wheels to perform drifting and sliding maneuvers. Drift trikes typically use the front wheel and steering system from a bicycle, the rear axle system from a go-kart, and a steel tube frame. Many drift trikes use special low-friction PVC or HDPE plastic sleeves to cover the rear wheels for the purpose of reducing traction. Originally, drift trikes were not motorized, and were primarily drifted through the curves of steep, hilly roads. More recently, drift trike builders have introduced motorized trikes which provide the same drifting experience on level ground. The majority of these motorized trikes are powered by internal combustion engines; however, a drift trike powered by an electric motor has some significant benefits over a gas-powered trike. The use of an electric powertrain eliminates emissions from the operation of the vehicle and provides high torque even at low speeds. However, there are few electric drift trikes commercially available, and those electric drift trikes do not have comparable power to their gas-powered counterparts. The objective of this project is to design and fabricate an electric drift trike with performance comparable to high-power combustion counterparts.

## Functional Requirements

At the beginning of the development of the drift trike, it was necessary to set functional requirements and performance benchmarks for the design of the trike. The functional requirements include:

1. Trike should break traction in the rear wheels from a standstill. This ensures that the trike has enough torque to perform the characteristic maneuvers of a drift trike including: burnouts, donuts, and drifts.
2. The trike should also be able to accelerate at the maximum rate allowed by the traction of the low-friction sleeves.
3. The expected top speed of the trike should be at least 25 miles per hour but should not exceed 35 miles per hour. This range of speeds should maximize rider enjoyment while not endangering the rider through excessive speed.
4. The operational time on a full battery charge should exceed 30 minutes at the maximum possible operating power of the trike.
5. The target weight for the trike is 150 pounds with capacity for a rider of up to 200 pounds.
6. The trike should not tip during operation, especially when performing tight-radius turns, meaning that the center of gravity of the trike and rider should be kept low to the ground.

These requirements informed design decisions throughout the trike’s development cycle.

## Drift Trike Components

In the construction of the drift trike, many different parts and subsystems are integral to the operation of the vehicle. The mechanical subsystems include:

- Tube frame
- Rear axle assembly
- Chain drive
- Rear braking system
- Front wheel, forks, and handlebars
- Front braking system
- Adjustable Seat

The electrical components include:

- Electric motor
- Motor controller
- Batteries
- Contactor
- Switches
- Throttle.

Each of these subsystems and components needed to be rigorously selected in order to meet the functional requirements of the overall trike. The selection of the motor, motor controller, and batteries will be reviewed in subsequent sections.

# Drift Trike Design

## Geometric Studies

In order to determine the trike's frame geometry, one of the most important considerations was the positioning and comfort of the vehicle's rider. The positions of the seat and handlebars especially would be important driving dimensions in the frame design and would also influence packaging and placement of the batteries and motor. Initial tests of seat, handlebar, and footrest positions were conducted using wooden blocks to simulate foot rests, using cushions to simulate a seat and using PVC pipes to simulate handlebars. The height, angle, and forward position of both the mockup handlebars and the foot rests were varied relative to the seat position.

*Figure 1: Seat and handlebar geometric prototyping*

Based on ergonomic testing, it was concluded that the height and forward position of the handlebars were critical in maintaining good posture and comfort for the rider. The positioning of the foot rests was also important, yet less dimensionally sensitive. Furthermore, it was important that the rider could reach both handlebar grips even at aggressive steering input angles. For a test rider of 5’7” in height, the optimal position of the handlebars was determined to be 23.5 inches above the seat height and 25.5 inches forward of the seat back. To accommodate different heights of riders, it was decided that an adjustable seat should be incorporated into the design. An adjustable seat sliding mechanism with a range of motion of 7 inches was added to the design to allow for the tuning of rider position to ensure rider comfort.

In addition to the use of physical mockups, a virtual mannequin was also constructed in Computer Aided Design software to verify trike geometry and to accurately model the rider’s center of gravity in the drift trike design. The mannequin was designed from proportional drawings of the human frame and scaled to 5’7” in height. The mannequin’s mass properties were adjusted to accurately model the contribution of the rider to the vehicle’s center of mass. Through the use of both physical and virtual mockups and prototypes, optimal positions for the seat and handlebars were determined.

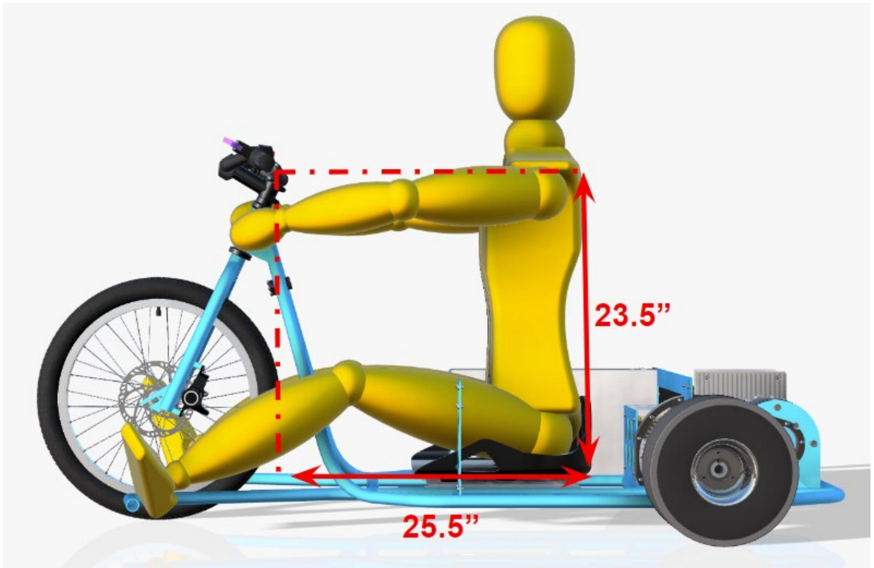

*Figure 2: Virtual mannequin in CAD model with dimensions for optimal handlebar placement*

## Coefficient of Friction

One other important step in the development of the trike was to determine the coefficient of friction of the plastic sleeves covering the rear wheels. HDPE sleeves were selected because they had better wear characteristics than PVC sleeves. Online sources for the coefficient of friction of HDPE did not include values for its coefficient of friction against paved surfaces, and especially not in a scuffed or worn condition. To accurately simulate trike performance in acceleration, to properly select an electric motor, and to determine a drivetrain ratio, it was important to first know the coefficient of friction of the HDPE material. Because the final HDPE sleeves had not yet been acquired, flat test sheets of HDPE were used in a variety of tests to determine the coefficient of friction on a paved surface.

One of the HDPE sheets was tested in its original (smooth) state, while the other HDPE sheet was scuffed on the pavement to simulate wear which the sleeves would experience during regular use. Each HDPE sheet was placed on a small slab of concrete, and a box for adding weights was affixed to the top of the sheet. The block was tilted manually, and a phone accelerometer was used to measure the tilt angle. Once the sheet began to slip, the angle at which it slipped was recorded. The slip angle was measured for each sheet at multiple values of added weights up to ~3kg with 3 trials at each weight. The coefficient of friction could be calculated from the slip angle through a basic calculation.

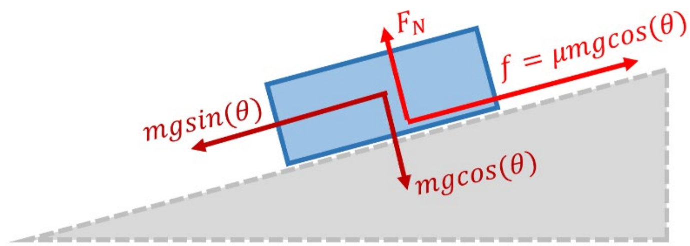


*Figure 3: Free body diagram of HDPE sheet on sloped concrete surface*

The forces in the direction parallel to the concrete surface are balanced then both sides of the equation are divided by $mgcos(\theta)$ to yield an equation for μ.

$$\mu mgcos(\theta) = mgsin(\theta)$$

$$\mu = \tan(\theta)$$

*Figure 4: Coefficient of friction experimental setup*

The experimental results for the test of the smooth and scuffed HDPE sheets are shown below:

| Weight (kg) | Slip Angle (1) | Slip Angle (2) | Slip Angle (3) | Average Angle |
|---|---|---|---|---|
| 0.278 | 21 | 15 | 16 | 17.33 |
| 1.262 | 20 | 15 | 14 | 16.33 |
| 1.714 | 16 | 14.5 | 14.5 | 15 |
| 2.2 | 17 | 15 | 14.5 | 15.5 |
| 3.094 | 16.5 | 16 | 15.5 | 16 |
| | | | Total Average Angle | 16.03 |
| | | | Coefficient | 0.29 |

*Table 1: Coefficient of friction tests for smooth HDPE on concrete surface*

| Weight (kg) | Slip Angle (1) | Slip Angle (2) | Slip Angle (3) | Average Angle |
|---|---|---|---|---|
| 0.276 | 27 | 30 | 28.5 | 28.5 |
| 1.258 | 24 | 21 | 20 | 21.67 |
| 1.716 | 19 | 19 | 17 | 18.33 |
| 2.2 | 25 | 19 | 22 | 22 |
| 3.092 | 17 | 16 | 15 | 16 |
| | | | Total Average Angle | 21.3 |
| | | | Coefficient | 0.39 |

*Table 2: Coefficient of friction tests for scuffed HDPE on concrete surface*

The scuffed sheet had a coefficient of friction of 0.39, which was significantly higher than the coefficient of friction for the smooth sheet. There was greater variance in the values for the scuffed sheet, likely because there are a larger number of possibilities for the contact between rough surface of the sheet and the rough surface of the concrete. Nevertheless, the coefficient for the scuffed sample of HDPE more closely matched the use case for the trike, so it was used in all subsequent calculations, especially the torque requirements for the motor selection.

The coefficient of friction was later verified once the sleeves had been acquired and mounted on the completed drift trike. In order to determine the weight on the back two wheels of the trike, the weight of the entire trike was measured at $880.6\ N$, and then the weight on the front wheel of the trike was measured at $163.8\ N$. Subtracting the front weight from the entire weight of the trike gave a total rear-axle weight of $716.9\ N$. This value would be used as the normal force between the rear wheels and the road for the purpose of the coefficient of friction calculation. To test the coefficient of friction of the sleeves on the rear wheels, the trike was set on a paved road surface with the front wheel aligned straight with the direction of motion of the trike. The rear brake lever was zip-tied in a fully depressed state to ensure that the rear axle was locked, and the rear wheels could only slip and not roll. A luggage scale was used to apply a pulling force to the center of the rear bumper, until the rear wheels slipped. The force as measured by the luggage scale at the instant which the rear wheels began to slip was recorded. The ratio between the slip force and the normal force would give the coefficient of friction between the sleeve and the pavement. This experiment was repeated for 5 trials, and then the results were averaged over these 5 trials.

| Normal Force (kg) | Slip force (kg) | Coefficient of Friction |
|---|---|---|
| 73.10 | 31.60 | 0.43 |
| 73.10 | 34.45 | 0.47 |
| 73.10 | 29.80 | 0.41 |
| 73.10 | 25.10 | 0.34 |
| 73.10 | 28.40 | 0.39 |
| | Average Coefficient of Friction | 0.41 |

*Table 3: Coefficient of friction tests for HDPE trike sleeves on paved surface*

The average calculated coefficient of friction was determined to be 0.41, which is approximately a 5% difference between the previously measured coefficient of friction of 0.39. The similarity in these experimental results validates that the motor torque calculations and acceleration simulations previously done are applicable to the performance of the trike as built.

## Motor Selection

In order to satisfy the requirements for the powertrain of the trike, the first component to be selected was the motor. The system voltage of 48 Volts had been previously selected because it was below the threshold of 50 volts, which is considered by OSHA to be the division between a low voltage system and a system with hazardous voltage requiring special training [1]. Thus, the specifications for all motors considered were reviewed at a voltage of 48 volts. To satisfy the performance benchmarks for the trike, the motor needed to provide a sufficient amount of torque to spin the rear wheels from a standstill, and to facilitate quick acceleration. The maximum acceleration rate allowed by the traction of the rear wheels is calculated based on the coefficient of friction for the sleeves: $\mu = 0.39$, the proportion of the trike weight on the rear axles: ~0.7, and the constant for gravitational acceleration: $g = 9.81\frac{m}{s^2}$.

$$F_{traction} = \mu * F_N = \mu * 0.7 * mg$$

$$F_{traction} = m * a$$

$$\mu * 0.7 * mg = m * a$$

$$a = \mu * 0.7g = 2.67\frac{m}{s^2}$$

By setting the equation for the traction force equal to the acceleration, it is determined that the frictional limitation on the trike's acceleration is equal to $2.67\frac{m}{s^2}$. Thus, the motor must be able to accelerate the trike at or very near this rate.

The maximum torque, $T_{max}$ which the rear axle could experience (as shown in Figure 5) given the traction limitations of the HDPE sleeves was calculated based on the weight on the rear wheels: $F_y = F_N = 170\ kg * 9.81\ \frac{m}{s^2} * 0.7 = 1223\ N$, the coefficient of friction: $\mu = 0.39$, and the radius of the wheel: : $r = 0.14\ m$.

$$T_{max} = \mu * F_N \times r = 66.65\ Nm$$

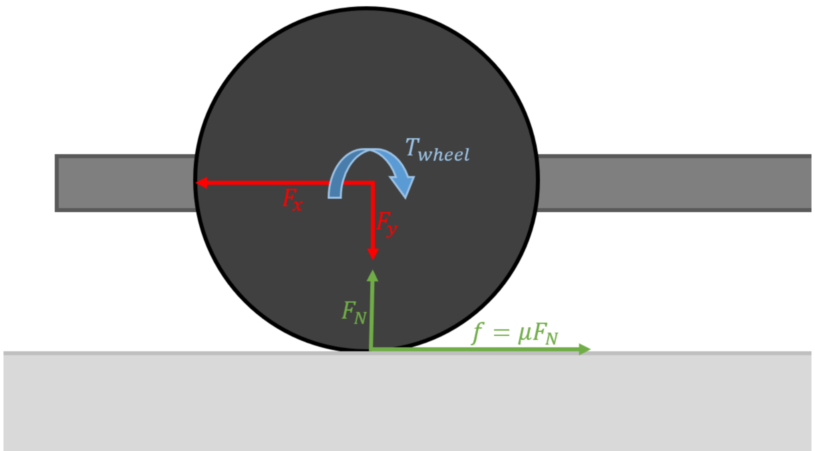


*Figure 5: Free body diagram of trike rear wheel*

The motor also needed to have sufficient maximum rotational velocity to achieve its target top speed. Both of these requirements for the motor were also influenced by the ratio of the chain drive which transmitted power from the motor output shaft to the rear axle of the trike.

Motors from the manufacturer, Motenergy, were considered, since they operated within the desired voltage range, torque range, and speed range; were readily available online; had previously been used in electric vehicle applications; and provided easily accessible performance specifications. Brushless motors were chosen rather than brushed motors since brushless motors have a higher power to weight ratio. Additionally, brushless motors are not susceptible to wear in consumable components such as graphite brushes. Two different models of brushless motors manufactured by Motenergy were considered. The ME1117 had higher torque than the ME1717 but a slightly lower speed than the ME1717 as can be seen in their torque-speed curves.

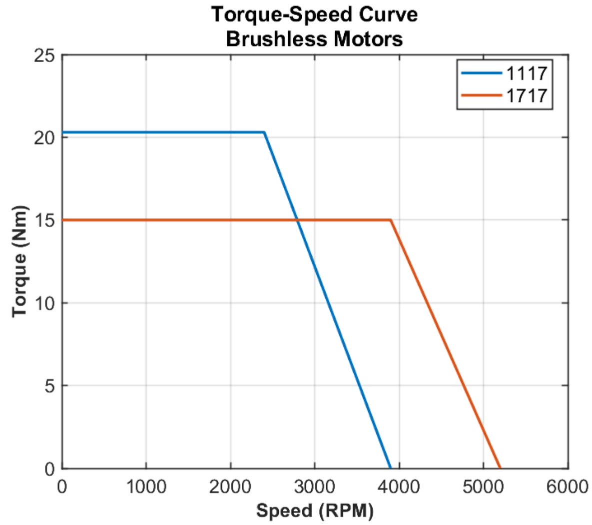


*Figure 6: Torque speed curves of ME1117 and ME1717 motors*

The motors were also compared using a performance simulation for the trike. The simulation used parameters including the trike's wheel size, mass, coefficient of friction, and coefficient of drag to simulate acceleration performance. It also allowed for the user to input differing torque-speed curves of different motors, and different sprocket ratios in the drivetrain. It is important to note that the simulation assumed that the rear drive wheels did not slip during acceleration, and that the actual acceleration of the trike could be no more than the calculated rate of to $2.67\frac{m}{s^2}$. The simulation was used to compare the acceleration performance of the ME1117 vs the ME1717, and to ensure that the trike would be to accelerate at the maximum rate allowed by the traction of the rear wheels.

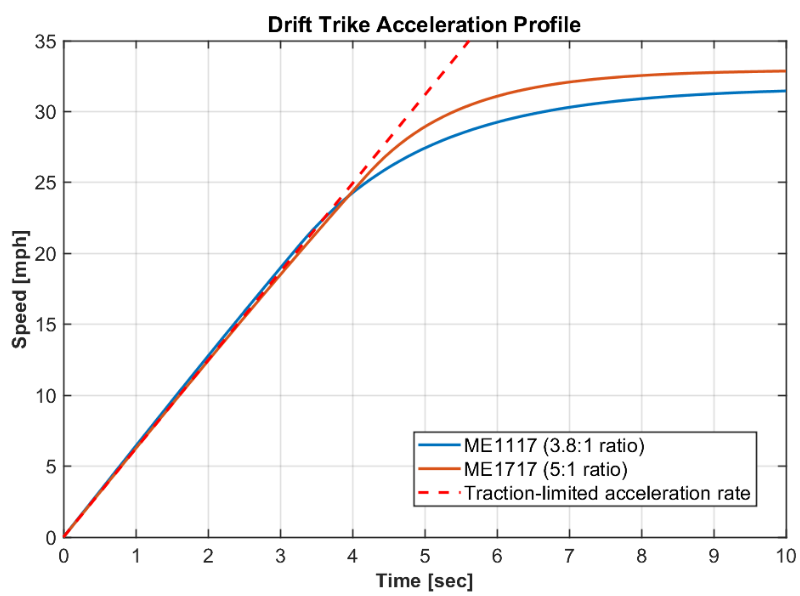


*Figure 7: Simulated acceleration profiles for ME1117 and ME1717 motors and theoretical maximum acceleration rate based on traction limitations of the rear wheels.*

Because the ME1117 had slightly more torque than the ME1717, it was optimal for the 1117 to have a chain drive ratio of 3.8:1, while it was optimal for the 1717 to have a ratio of 5:1. With these chain drive ratios, both had very similar acceleration profiles, with the 1117 accelerating slightly above and the 1717 slightly below the traction-limited acceleration rate. Also, the 1717 reached a slightly higher top speed than the 1117. While the acceleration performance was quite comparable, it was preferable to select the motor with the 3.8:1 chain drive ratio. For the diameter of the output shaft on both motors a 15-tooth sprocket was the smallest sprocket which was available in the correct chain pitch. The 5:1 ratio would have required a 75-tooth sprocket mounted to the rear axle, whereas the 3.8:1 ratio would have only required a 57-tooth sprocket mounted to the rear axle. Given the relative size of the rear wheels and the sprocket, a 75-tooth sprocket would have protruded below the frame of the drift trike, decreasing the ground clearance. Thus, it was more beneficial to select the motor which would require the 3.8:1 drive ratio. Therefore, the final motor selection was the Motenergy ME1117 motor. According to simulation results assuming minimal slippage, the ME1117 could accelerate to the benchmark speed of 25 mph within a time span of 4.2 seconds. The trike would also reach a top speed of 31.5 mph. The ME1117 motor has a continuous current draw specification of 100 Amps and the peak current draw of 300 Amps for 1 minute; however, since $T_{max} = 66.65\ Nm$ and the drive ratio is 3.8, the maximum torque which the motor would experience is only 17.5 Nm, which results in a current draw of only approximately 160 amps, based on the dynamometer plots for the ME 1117 attached in Appendix II.

## Controller Selection

The next component of the powertrain system to be selected was the motor controller. The motor controller would need to be compatible with a 3-phase brushless motor and would need to interface with the output of the motor's sine/cosine encoder. The motor controller should also operate at the nominal system voltage of 48V and should fully support the current which the motor would draw. The maximum motor current draw for the ME1117 motor was a continuous current draw of 100 Amps and the peak current draw of 300 Amps for 1 minute. The motor controller which was selected was a Sevcon Gen 4 Size 2. The Sevcon controller series was intended for use with brushless 3 phase motors, and the model selected operated at the nominal voltage of 48V. The controller also provided sufficient current capacity to drive the motor at its maximum current state. The Size 2 controller supported a peak current draw of 275 Amps for 2 minutes, and a continuous current draw of 110 Amps [2]. The controller satisfied the power requirements for driving the motor, but it also provided many beneficial features for the use case. The controller included multiple digital inputs which could be configured to include a safety switch, forward/reverse switches, and multiple drivability modes. The controller also integrated the precharge circuit for driving a DC line contactor from an on/off switch. Thus, the controller has sufficient power to drive the selected motor, and it provides many features which suit the use case of a drift trike.

## Battery Selection

To store the energy required to power the motor and motor controller, it was necessary to select the proper batteries for the drift trike system. The batteries would need to be matched to the operating voltage of the system of 48 volts. Additionally, the batteries would need to provide sufficient current capacity to the motor for it to perform at its maximum power state. Lastly, the batteries would need to provide sufficient energy capacity for the trike to operate for at least 30 minutes. The initial plan was to construct a custom battery pack from 18650 cells with a custom BMS and a custom enclosure. However, due to time constraints, and the donation of a sponsor, it was decided to use off the shelf battery modules supplied by NEC. The NEC battery modules are the ALM 12V35i HP, which is a 12 volt, 35 amp hour battery constructed from lithium-iron-phosphate cells. The battery pack for the trike is constructed from four 12 volt modules connected in series, which results in a nominal pack voltage of 48V. Each NEC battery module has a continuous discharge current of 210 amps, and a peak discharge current of 250 amps. While 250 amps does not match the rated peak current of the motor or the motor controller, since $T_{max} = 66.65\ Nm$ and the drive ratio is 3.8, the maximum torque which the motor would experience is only 17.5 Nm, which results in a current draw of only approximately 160 amps, based on the dynamometer plots for the ME 1117 attached in Appendix II. Thus, the current demand from the motor would never exceed the continuous current limit of the batteries.

The available energy within each NEC battery module is 462 Wh, which leads to a total battery pack energy of 1.8 kWh. Based on simulations of the trike power consumption, as shown in Figure 8, the dissipated power from rolling resistance and air resistance at the top speed was 0.95 kW.

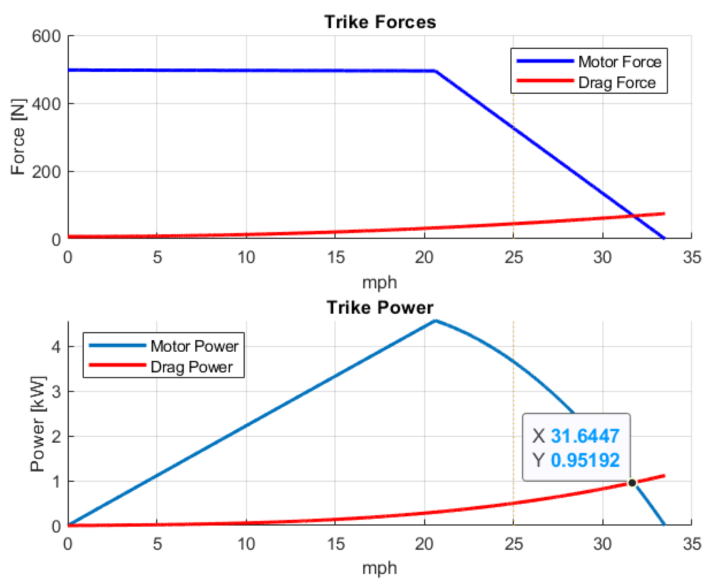


*Figure 8: Simulated power output and power consumption of trike throughout range of operational speeds*

By dividing the pack energy by the power consumption at top speed, the resultant operational time is 1.9 hours. It is important to note that the use case in which the user is accelerating frequently will result in a greater power draw and energy usage, than the case in which the trike is operating at its top speed for a prolonged period of time. Nevertheless, operational time of 1.9 hours gives a significant margin over the functional requirement of 0.5 hours of battery life. The four battery modules also fit nicely along the outside edges of the trike, which allows the design to maintain a low center of gravity for the trike and the rider. The NEC battery modules selected meet all the criteria for nominal voltage, current capacity, and battery life as outlined in the functional requirements for the trike.

## Electrical System Architecture

The electric system and wiring harness of the trike was constructed with considerations for the performance of the trike and the safety of the rider. The 48V battery can be disconnected from the trike system via an Anderson Powerpole connector. In order to power on the motor controller, a key switch must be turned which activates a precharge circuit within the motor controller to close a high current contactor on the positive lead from the battery. Once the motor controller is powered on, an enable switch on the handlebars must be closed to allow the controller to be active. Then the direction switch must be pressed in order to select the forward or reverse direction. Lastly, the throttle switch must be activated before the throttle input will be delivered to the motor. The throttle switch is a normally open switch which is closed when the throttle is twisted slightly. Thus, the throttle input voltage is only considered when the rider is actively twisting the throttle. This protects against a stuck throttle situation if there were to be a wiring fault in the throttle potentiometer. During the startup sequence for the trike, the key switch, enable switch, and directional switch must be pressed for the trike to be activated. When the trike is parked, the trike can be deactivated by the user by setting the directional switch to neutral, switching off the enable switch, and/or turning the key switch. This redundancy in switches ensures that the trike system is safe from accidental activation so long as the rider deactivates the trike promptly upon parking. The system architecture of the rider interface and powertrain can be seen in the wiring diagram in Figure 9 below.

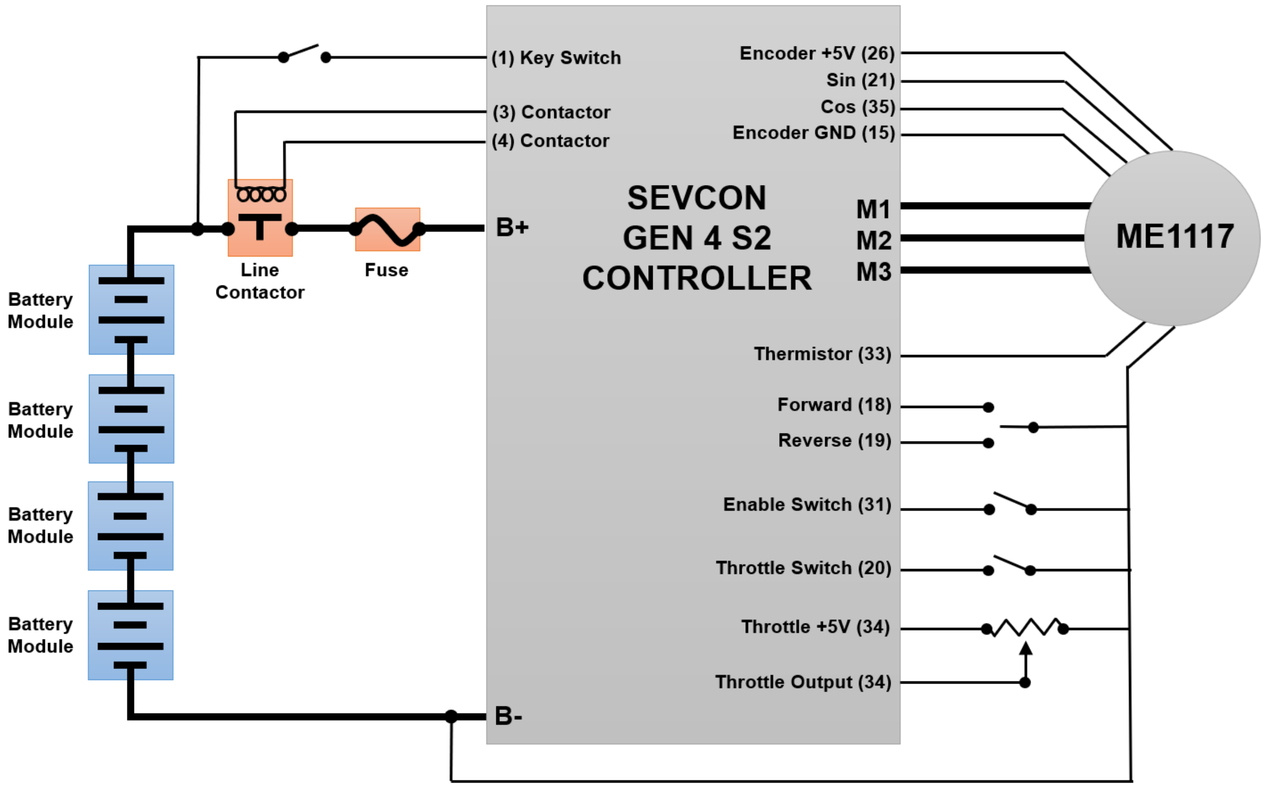


*Figure 9: Wiring diagram of drift trike electrical system*

# Conclusion

To conclude, powertrain components were selected which met the functional requirements and performance specifications for the trike. Driving geometrical relations for the trike's frame were set based on experiments in rider posture and comfort. The coefficient of friction for the drive wheels was measured to inform powertrain design decisions. This measurement was initially done with preliminary samples of the material and was validated with measurements of the coefficient of friction for the drive wheels of the trike.  A motor and chain drive ratio were selected which met the criteria for the maximum acceleration rate and maximum speed. A motor controller and battery system were selected to match the system voltage and to provide sufficient current to the drive motor. System architecture and safety features of the trike's electrical system were developed to ensure safety of the trike operation. The drift trike was fabricated and assembled as seen in Figure 10. The completed trike meets all the functional requirements.

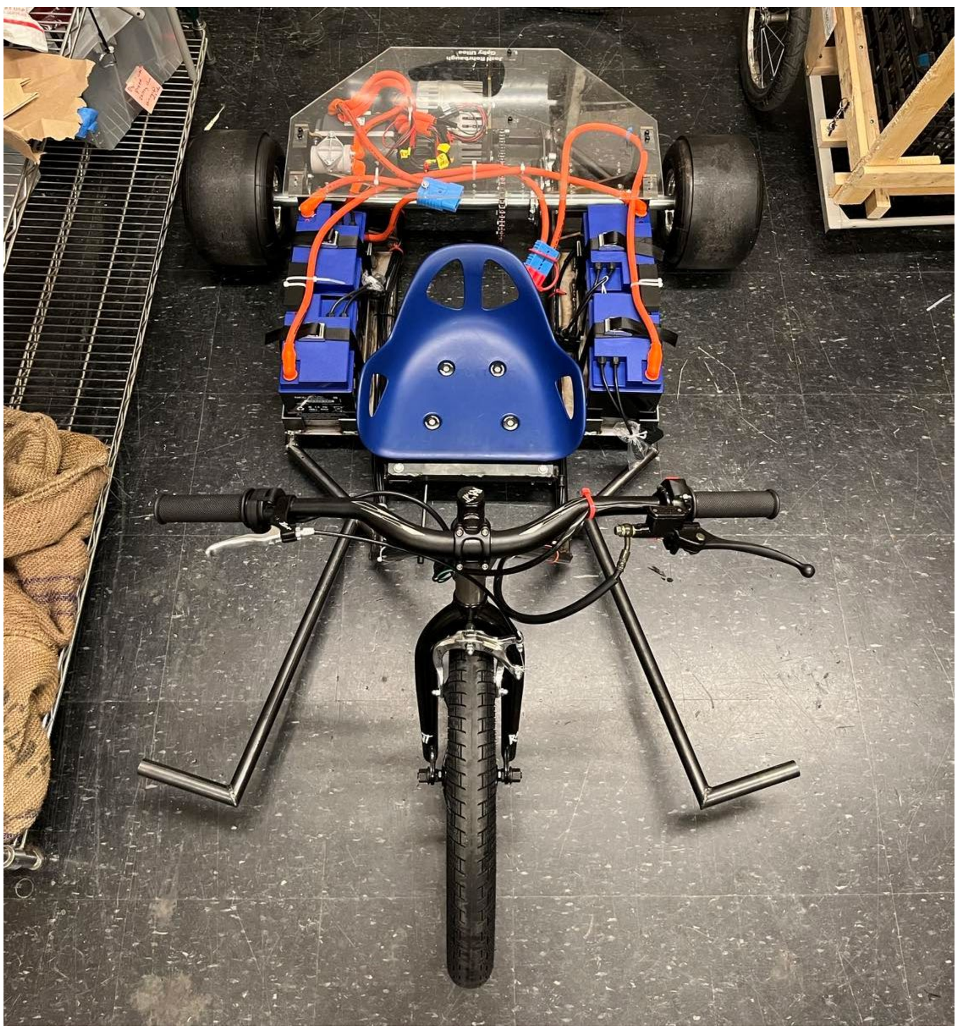

*Figure 10: Photograph of completed trike*

## References


[1] “Safety and Health Regulations for Construction: Electric Power Transmission and Distribution.” 1926.960 - Working on or near exposed energized parts. | Occupational Safety and Health Administration, October 5, 2015. https://www.osha.gov/laws-regs/regulations/standardnumber/1926/1926.960.

[2] Sevcon Ltd. “Gen4 Applications Reference Manual.” Gen4 product manual . Accessed May 11, 2023. https://www.thunderstruck-ev.com/images/Gen4%20Product%20Manual%20V3%204.pdf. [3] NEC Battery Data Sheets

[3] “ALM 12V35 Datasheet.Pdf.” NEC Energy Solutions, 2015. https://www.nec-battery.de/_media/PDF/ALM%2012V35%20Datasheet.pdf.

# Appendix I: Motor Dynamometer Plots

## ME1117 Dynamometer Plot

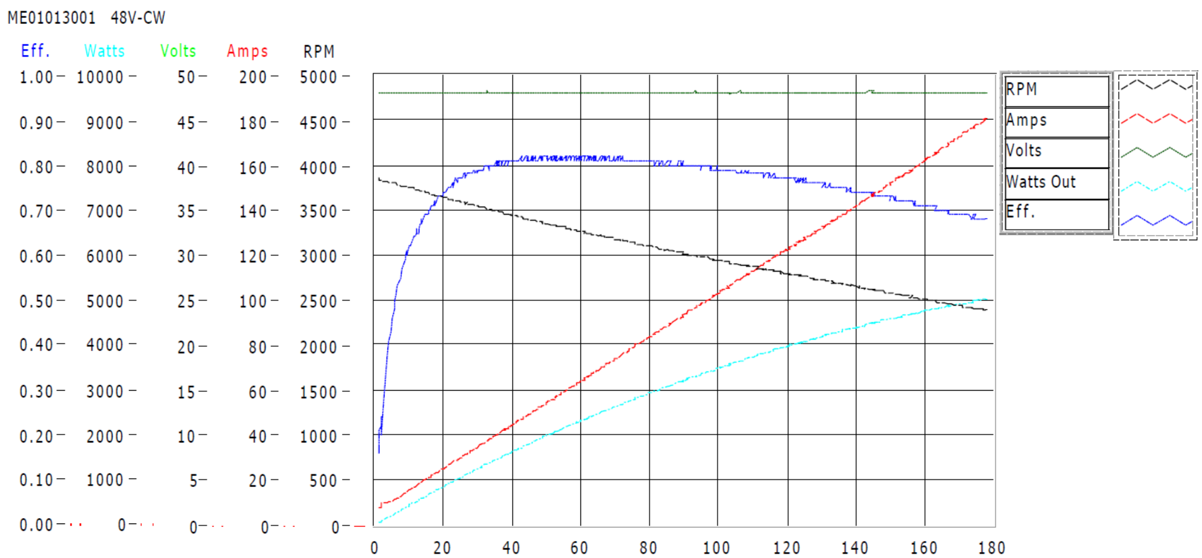


Dynamometer plot for ME1117 motor performance at 48 V as measured by Motenergy Inc.

## ME1717 Dynamometer Plot

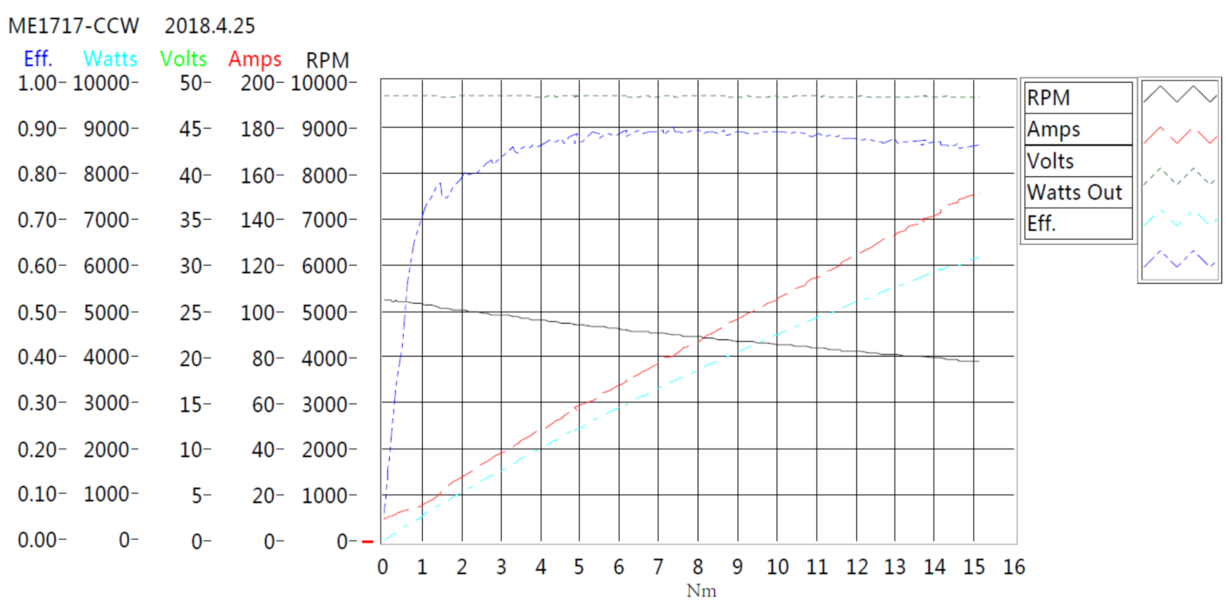


Dynamometer plot for ME1717 motor performance at 48 V as measured by Motenergy Inc.

# Appendix II: Simulation Matlab Code

## Simulink Model for Trike Acceleration

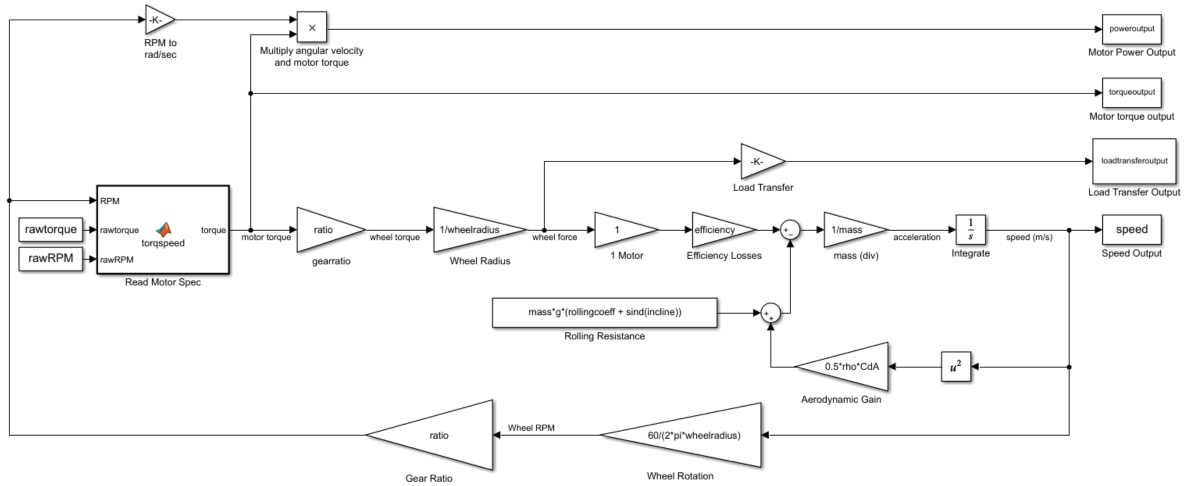


## Matlab Model of Trike Performance

```
%% Geometric Parameters

%Drift Trike Parameters

FrontWheel = 20; %[in] Front wheel diameter
RearWheel = 11; %[in] Rear Wheel diameter
wheelbase = 43.6; %[in]
track = 38; %[in]
CG = [wheelbase - 11.534,10.995]; %[in]

wheeldiameter = 0.0254*RearWheel; %[m] diameter of wheel
wheelradius = wheeldiameter/2; % [m] radius of wheel

vehicle_mass = 100; %[kg] vehicle mass
rider_mass = 70; %[kg] rider mass
mass = vehicle_mass+rider_mass; %[kg] total mass
g = 9.81; %[N/kg] gravity

rollingcoeff = 0.004; %rolling resistance of bicycle tires
A = 0.25; %frontal area of bike (m^2)
CdA = 0.5; %from a Kawasaki ZX-10R in elmoto.net
rho = 1.2; %density of air kg/m3


%%%%%%%%%% Performance Objectives %%%%%%%%%%%%
maxSpeed = 25; %[mph]
```

```
%% Drivetrain Configuration

%Drivetrain Configuration
ratio=(57/15); %gear ratio (axle sprocket/motor sprocket)
efficiency = 0.90; %assume 90% efficiency for chain drive

% ME1117 specs based on dyno plot for ME0907 at 48V (same motor) but
% different encoder
rawtorque=[20.3,20.3,0];; %torque in Nm (can do 38 peak but only 22
continuous)
rawRPM=[0,2400,3900]; %rpm from torque graph

RPM= 0:rawRPM(3);
torque=interp1(rawRPM,rawtorque,RPM,'Linear','extrap');

figure
hold on
grid on
plot(RPM,torque,'linewidth',2)

title({'Torque-Speed Curve','ME1717'})
xlabel('Speed (RPM)')
ylabel('Torque (Nm)')

%% Vehicle Forces

v=(1/ratio)*(RPM/60)*pi*wheeldiameter; %metre per second of trike
mph=2.23*v; %velocity in mph

%positive forces
wheeltorque = torque*ratio*efficiency; %force the motor is putting out in N @
wheel
motorforce = wheeltorque/wheelradius;

%negative forces
dragforce=0.5*v.^2*rho*CdA; %force of drag in [N]
rollingforce=rollingcoeff*mass*g; %rolling resistance
resistance = (dragforce+rollingforce); %total drag

%powers
motorpower=motorforce.*v/1000; %power by motor [kW]
dragpower=resistance.*v/1000; %power dissipated by drag [kW]


%% Force & Power vs. Speed Graphs
%close all

figure
subplot(2,1,1)
hold on
grid on
```

```
plot(mph,motorforce,'b','LineWidth',2)
plot(mph,resistance,'r','LineWidth',2);
plot([maxSpeed, maxSpeed],[min(motorforce),max(motorforce)],':')
legend('Motor Force','Drag Force','location', 'NorthWest')
xlabel('mph')
ylabel('Force [N]')
title('Trike Forces')

subplot(2,1,2)
hold on
grid on
plot(mph,motorpower,'LineWidth',2)
plot(mph,dragpower,'r','LineWidth',2)
plot([maxSpeed, maxSpeed],[min(motorpower),max(motorpower)],':')
%plot([0 20],[.66 .66],'k--','LineWidth',2)
legend('Motor Power','Drag Power','location', 'NorthWest')
title('Trike Power')
xlabel('mph')
ylabel('Power [kW]')


%% Acceleration Profile

%Drift Trike Parameters

FrontWheel = 20; %[in] Front wheel radius
RearWheel = 11; %[in] Rear Wheel radius
wheelbase = 43.6; %[in]
track = 38; %[in]
CG = [wheelbase - 11.534,10.995];

wheeldiameter = 0.0254*RearWheel; %[m] diameter of wheel
wheelradius = wheeldiameter/2; % [m] radius of wheel

mass= 100; %[kg] vehicle weight
rider = 70; %[kg] rider weight
mass = mass+rider;
g=9.81; %[N/kg] gravity

rollingcoeff=0.004; %rolling resistance of bicycle tires
A=.25; %frontal area of bike
CdA=0.5; %from a Kawasaki ZX-10R in elmoto.net
rho=1.2; %density of air kg/m3

%%%%%%%%%% Performance Objectives %%%%%%%%%%%%
maxSpeed = 25; %[mph]
incline = 0; %[deg]

ratio = 57/15; %gear ratio (Hub Motor)
efficiency = 0.90;
% ME1305
```

```
rawtorque=[20.3,20.3,0]; %torque in Nm
rawRPM=[0,2400,3900]; %rpm from torque graph
RPM= 0:rawRPM(3);
torque=interp1(rawRPM,rawtorque,RPM,'Linear','extrap');

wheelradius = 11*0.0254/2;
sim('TrikeAccelerationModelConsolidated1305.slx')
maxspeed=(max(speed.Data)*2.23);
speedMPH = speed.Data*2.23;
time = speed.Time;

figure
hold on
grid on
plot(speed.Time,speedMPH,'LineWidth',2);
plot([0,max(speed.Time)],[maxSpeed,maxSpeed],'-.')
title({'1117 Acceleration Profile'}, 'FontSize', 22)
ylabel('Speed [mph]', 'FontSize', 20)
xlabel('Time [sec]', 'FontSize', 20)
```